ROMAI J., v.10, no.2(2014), 65–74

ANISOTROPIC METRIC MODELS IN THE GARNER ONCOLOGIC FRAMEWORK

Vladimir Balan[1], Jelena Stojanov[2]
[1] *University Politehnica of Bucharest, Romania*
[2] *University of Novi Sad, Zrenjanin, Serbia*
vladimir.balan@upb.ro, jelena@tfzr.uns.ac.rs

Abstract The present paper considers Finslerian model related to the classical Garner dynamical system, which models the cancer cell population growth. Certain locally-Minkowski anisotropic structures are statistically built for differently dense grids of samples. The geometric background and compatibility with the dynamical system are discussed.
Work presented as invited lecture at CAIM 2014, September 19-22, "Vasile Alecsandri" University of Bacău, Romania.

Keywords: dynamical system, statistical fitting, Finsler structure.
2010 MSC: 53B40, 37C75, 37C10, 37E30.

1. INTRODUCTION

Recently, a large number of applications emphasize the role of anisotropic geometric structures in modeling real-life phenomena (e.g., [2, 9, 5]). By applying a statistical technique similar to the one used in [2], we shall construct three locally-Minkowski Finslerian structures suitable for the Garner dynamical system of cancer cell population. The structures of Randers, Euclidean and 4-root type, which are built on the system data, provide information on the evolution of the cancer cell population ([6]). All the three metric tensor fields related to the fit structures are elements of the Hilbert space of bounded and continuous $(0, 2)$-type d-tensors [9, 14]. The canonic Euclidean metric δ is used to compare Finsler metrics within the Hilbert space and to evaluate their norms. The comparison between the Randers and Euclidean type norms was performed in [6, 7]. The goal of this work is to investigate the relevance of the grid density towards the resulting Finsler-type structures.

2. THE GARNER DYNAMICAL SYSTEM

The subpopulations of abnormal cells responsible for the cancer disease contain the so called *cancer stem cells* (CSCs), [15]. In this context, it is very important to describe changes in the cancer population, which contains three types of cells, [11, 13]: proliferating, quiescent (resting) and dead ones, their abundance being determinant in the prognostic of the cancerous disease.

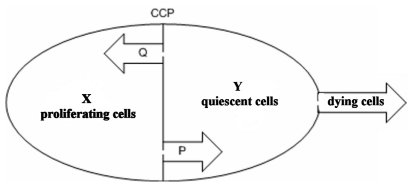

Fig. 1.: Transitions between the cell classes in the Solyanik and Garner cancer evolution models

The evolution of the cancer cells population was firstly modeled in 1995 by means of Solyanik's dynamical system [16], and further improved by Garner et al. in [12]. The Garner dynamical system describes the evolution of the amounts of the quiescent and proliferating cells:

$$\begin{cases} \dot{x} = x - x(x+y) + \dfrac{hxy}{1+kx^2} \\ \dot{y} = -ry + ax(x+y) - \dfrac{hxy}{1+kx^2}, \end{cases} \tag{1}$$

where:

- $x = \frac{c}{b}\tilde{x}$ and $y = \frac{ca}{b}\tilde{y}$ are scaled amounts of the population cells, and $\tilde{x}$ and $\tilde{y}$ are numbers of proliferating and quiescent cells respectively;
- a measures the relative nutrient uptake by resting vs. proliferating cancerous cells;
- c gives the magnitude of the rate of cell transition from the proliferating to the resting state;
- $\bar{A}$ is the initial rate of the increase at small $\tilde{x}$ of the intensity of cell transition from quiescent to proliferating state;
- $\bar{A}/\bar{B}$ is the rate of the decrease for large $\tilde{x}$ of of the intensity of cell transition from quiescent to proliferating state;
- $r = d/b$ is the ratio between the death rate of quiescent cells and the birth rate of proliferating cells;
- $h = \bar{A}/(ac)$ represents a growth factor that preferentially shifts cells from quiescent to proliferating state;
- $k = \bar{B} \cdot (b/c)^2$ represents a mild moderating effect.

Figure 1 shows the influence of the parameters on the change in the nature of cancer cells in the population of a cancerous tissue.

The associated nullclines, equilibrium points, the appropriate versal deformation and the static bifurcation diagram of the Garner system were studied in [3, 4].

When in the original GS system (1) the constant $h = \bar{A}/(ac)$ is negligible ($0 < |h| \ll 1$) or vanishes, one obtains the reduced dynamical system (further denoted as RS)

$$\begin{cases} \dot{x} = x - x(x+y) \\ \dot{y} = -ry + ax(x+y). \end{cases} \tag{2}$$

In the original system GS, for significant values of h, one notices a malignant evolution of the illness, which happens when the parameter a becomes negligible (this might happen due to a small ratio of nutrient uptake of resting vs. proliferating cells, which shows that the resources are absorbed mostly by the proliferating cells in the detriment of quiescent cells), due to the fact that the parameter c might be negligible (in such a case, the rate of cell transition from cancerous to the resting state is negligible, and hence the evolution of the disease is either stationary, or worsening), or in the case when the parameter $\bar{A}$ significantly increases (then the rate of increase of Q is abruptly big at small x, i.e., the cell transition from the quiescent to cancerous cells is intense).

We conclude that when these conditions are far from being achieved, i.e., when the evolution of the disease is controlled (for $0 \leq |h| << 1$), then GS (1) can be approximated by RS (2).

3. FINSLERIAN STRUCTURES

A Finsler space is a differential manifold M endowed with the fundamental function F (Finslerian norm), defined as follows ([8, 10, 9])

Definition 3.1. *A real scalar function $F : TM \to [0, \infty)$ is called a* Finsler fundamental function *if it satisfies the following properties:*

1 *F is smooth on the slit tangent space $TM \setminus \{0\} = \{(x, y) | x \in M, y \in T_xM, y \neq 0\}$ and is continuous on the image of the null section of the tangent bundle (TM, π, M);*

2 *F is positively 1-homogeneous in the directional argument, i.e., $F(x, \lambda y) = \lambda F(x, y), \quad \forall \lambda > 0$;*

3 *the smooth maps $g_{ij} : TM \setminus \{0\} \to \mathbb{R}$, $i, j \in \overline{1, n}$ given by*

$$g_{ij} = \frac{1}{2} \frac{\partial^2 F^2}{\partial y^i \partial y^j}, \tag{3}$$

form the symmetric positive definite matrix, $[g] = (g_{ij})_{i,j \in \overline{1,n}}$, and are the components of the Finsler metric tensor field *$g = g_{ij} dx^i \otimes dx^j$.*

Also, in the case when $[g]$ is not positive definite, but non-degenerate, and with constant signature, then (M, F) is called pseudo-Finsler structure *[5].*

The fundamental metric $g = g_{ij}(x, y) dx^i \otimes dx^j$ of a Finsler manifold is a d-tensor on the tangent space [8, 10].

We shall consider extensions of this definition, by assuming that the domain of F is a strict subset of TM, and that the operations within the fibres are feasible. A significant geometric object derived from the Finsler structure is the Cartan tensor [8, 9, 10],

$$C_{ijk} = \frac{1}{2} \frac{\partial g_{ij}}{\partial y^k} = \frac{1}{4} \frac{\partial^3 F^2}{\partial y^i \partial y^j \partial y^k}. \tag{4}$$

This is a $(0,3)$-type, totally symmetric d-tensor on the tangent space and it is positively homogeneous of order -1. It reflects the non-Riemannian nature of the structure, since the Finsler metric tensor field reduces to a Riemannian one if and only if the Cartan tensor vanishes.

Both the Finsler metric g_{ij} and the Cartan tensor field C_{ijk}, depend on the tangent space coordinates (x, y), and belong to Hilbert spaces of (bounded and continuous) d-tensor fields of the corresponding type, $(0,2)$ and $(0,3)$, respectively [9, 14]. Generally, the scalar product which provides the Hilbert structure generally acts on a pair of two $(0,m)$-tensors $\mathcal{A}$ and $\mathcal{B}$ by means of the formula:

$$\langle \mathcal{A}, \mathcal{B} \rangle_h = \mathcal{A}_{i_1 \dots i_m} h^{i_1 j_1} \dots h^{i_m j_m} \mathcal{B}_{i_1 \dots i_m},$$

for a given regular metric $(0,2)$-tensor with components h_{ij}. In this work we use the canonical Euclidean metric $h = \delta$, which naturally allows to evaluate the norm of the Finsler metrics,

$$||g|| = \sqrt{\langle g, g \rangle_\delta} = \sqrt{Trace(g_{ij} g^{jk})}. \tag{5}$$

In order to compare the corresponding Cartan tensors, we use the Frobenius norm

$$||C||_g = \sqrt{C_{ijk} g^{ir} g^{js} g^{kt} C_{rst}}. \tag{6}$$

The Finsler fundamental functions considered in [6, 7] and in this work are chosen to be of locally Minkowski type. This infers that the numerous related to them geometric objects considerably simplify: the geodesics are (pieces of) straight lines, the KCC invariants vanish, the Berwald linear connection is trivial [1, 9]. In fact, the Finsler structures will provide point-independent norms, Finsler norms of the Minkowski type. We shall determine by statistical fitting three such norms, having the following prescribed forms:

$$F_R(y) = \sqrt{\delta_{ij} y^i y^j} + b_i y^i = \sqrt{(y^1)^2 + (y^2)^2} + b_1 y^1 + b_2 y^2, \tag{7}$$

$$F_E(y) = \sqrt{c_1 \cdot (y^1)^2 + c_2 \cdot y^1 y^2 + c_3 \cdot (y^2)^2}, \tag{8}$$

$$F_Q(y) = \sqrt[4]{q_1 \cdot (y^1)^4 + q_2 \cdot (y^1)^3 y^2 + q_3 \cdot (y^1)^2 (y^2)^2 + q_4 \cdot y^1 (y^2)^3 + q_5 \cdot (y^2)^4}, \tag{9}$$

where the real constants $b_{1,2}$, $c_{1,2,3}$ and $q_{1,2,3,4,5}$ are parameters of the three Finsler structures.

4. SAMPLING AND STATISTICAL FITTING

The basic assumption in this work is that both systems, the Garner and the reduced ones, have grossly resembling field lines. The main idea of the fitting is determine by least-squares fitting the coefficients of prescribed-type Finslerian norms, numerically given by the Euclidean norm of the slightly shifted velocity vector. The constructing process of the measuring Finslerian tool is presented in the following scheme:

$$\begin{tikzcd}
 & D \arrow[rr, "\|\cdot\|_F"] \arrow[dl, shift left, "\pi_1"] \arrow[dr, shift left, "\pi_2"] & & \mathbb{R} & \\
K_1 \arrow[ur, shift left, "\sigma_1=X_R|_{K_1}"] \arrow[dr, hook] & & K_2 \arrow[ul, shift left, "\sigma_2"] \arrow[rr, "X_G"'] \arrow[dl, hook'] & & V \arrow[ul, "\|\cdot\|_E"'] \\
 & K & & &
\end{tikzcd}$$

The configuration space of the Garner dynamical system (and of the reduced system, as well) is a bounded subset of $K \subset K_+ = \{p = (x, y) \mid x > 0, y > 0\} \subset \mathbb{R}^2$, containing a large class of possible states. The field lines of the reduced system (2), which is considered for the parameter values $a = 1.998958904$ and $r = 0.03$ (see [12]), yield a vector subset D of the tangent space TK_+, containing related feasible directions $\dot{p} = (\dot{x}, \dot{y}) \in T_pK_+$. By using the theorem of inverse function, the polynomial form of the reduced system enables a reverse association $\dot{p} = (\dot{x}, \dot{y}) \rightsquigarrow p = (x, y)$, given by the second of the possible reverse mappings σ_1 and σ_2. Precisely, the second degree of the polynomials yields two p-domains, the subsets $K_{1,2} \subset K_+$, of which we choose just one in the statistical fitting. Further, by using the Garner vector field X_G with the parameter values $h = 1.236$ and $k = 0.236$ ([3, 12]), we associate to the detected point $p = (x, y)$ (and hence, to the initial vector $\dot{p} \in D$, the corresponding shifted vector $\dot{p}_e \in V$.

The super-determined linear system which gives the coefficients of the Finsler norm is

$$\|\dot{p}\|_F = \|\dot{p}_e\|_E. \tag{10}$$

The discretization is achieved by a grid spanned over the coordinates of the feasible directions over the p-domain K_2 and V:

$$\begin{tikzcd}
Gr(D) \arrow[r, "\|\cdot\|_F"] \arrow[d, "\pi_2"'] & \mathbb{R} \\
Gr(K_2) \arrow[r, "\sigma"'] & Gr(V) \arrow[u, "\|\cdot\|_E"']
\end{tikzcd}$$

The grid defines a discrete sample volume N, and leads to the approximation problem (10), which produces the system of linear equations in the unknown parameters of the Finsler structure. The three Finsler structures of Randers, Euclidean and 4-root type, which are related to the Garner oncologic framework live on the 2-dimensional configuration space, and depend on parameter-coefficients, as follows:

$$F_R(\dot{x}, \dot{y}) = \sqrt{\dot{x}^2 + \dot{y}^2} + b_1\dot{x} + b_2\dot{y}, \tag{11}$$

$$F_E(\dot{x}, \dot{y}) = \sqrt{c_1\dot{x}^2 + c_2\dot{x}\dot{y} + c_3\dot{y}^2}, \tag{12}$$

$$F_Q(\dot{x},\dot{y}) = \sqrt[4]{a(\dot{x})^4 + b(\dot{x})^3(\dot{y}) + c(\dot{x})^2(\dot{y})^2 + d(\dot{x})(\dot{y})^3 + e(\dot{y})^4}. \tag{13}$$

The corresponding over-determined linear systems ($k \in \overline{1,N}$, $N >> 5$) are

$$b_1\dot{x}_k + b_2\dot{y}_k = \sqrt{(\dot{x}_e)_k^2 + (\dot{y}_e)_k^2} - \sqrt{\dot{x}_k^2 + \dot{y}_k^2}, \tag{14}$$

$$c_1\dot{x}_k^2 + c_2\dot{x}_k\dot{y}_k + c_3\dot{y}_k^2 = (\dot{x}_e)_k^2 + (\dot{y}_e)_k^2, \tag{15}$$

$$a(\dot{x})_k^4 + b(\dot{x})_k^3(\dot{y})_k + c(\dot{x})_k^2(\dot{y})_k^2 + d(\dot{x})_k(\dot{y})_k^3 + e(\dot{y})_k^4 = \left((\dot{x}_e)_k^2 + (\dot{y}_e)_k^2\right)^2, \tag{16}$$

and allow to statistically fit the values $b_{1,2}$, $c_{1,2,3}$ and a, b, c, d, e by the method of least squares.

We note that the uniform grid over the domain of the feasible directions provides the needed inputs for the fitting process. Maple computation produces the corresponding polar (ρ,θ)-domain of the field lines of the Garner system,

$$I_\rho \times I_\theta = [0.329915, 0.888939] \times [1.0988, 1.51452],$$

a grid with $N = (n_\rho + 1)(n_\theta + 1)$ knots

$$(\rho_i, \theta_j) \in I_\rho \times I_\theta,\ (i,j) \in \overline{0,n_\rho} \times \overline{0,n_\theta}.$$

The Cartesian domain of the feasible directions is

$$\varphi(I_\rho \times I_\theta) = I_1 \times I_2 = [0.05, 0.1596] \times [0.293844, 0.887532],$$

and the used grid consists of scaled spherical harmonics regarded as tangent vectors

$$\dot{p}_k = (\dot{x}_k, \dot{y}_k) = (\rho_i \cos\theta_j, \rho_i \cos\theta_j) \in D = I_1 \times I_2, \quad k \in \overline{1,N}$$

where $k = (i-1)n_\rho + j \in \overline{1,N}$.

5. THE GARNER MODEL GEOMETRIC STRUCTURES

5.1. THE RANDERS STRUCTURE

By considering first $n_\rho = n_\theta = 5$, the grid produces $N = 6^2$ samples and the least square method yields the structure

$$F_{R_6}(\dot{x},\dot{y}) = \sqrt{\dot{x}^2 + \dot{y}^2} + b_1\dot{x} + b_2\dot{y}, \quad \begin{cases} b_1 = 0.6284819877782055l8 \\ b_2 = -0.269476980932055964\,. \end{cases} \tag{17}$$

A denser grid, with $N = 11^2$ samples ($n_\rho = n_\theta = 10$), leads to

$$F_{R_{11}}(\dot{x},\dot{y}) = \sqrt{\dot{x}^2 + \dot{y}^2} + b_1\dot{x} + b_2\dot{y}, \quad \begin{cases} b_1 = 0.629387435652307036 \\ b_2 = -0.269842591353006478\,. \end{cases} \tag{18}$$

The difference between the two output Randers norms is linear. The metrics are positively definite in both cases and their corresponding quadratic forms for the flagpole $(0.1, 1)$ differ by a smooth function, see Fig. 2.

By the use of (5) and (6), we compare the main geometric objects. Namely, the norm shift of the two metric tensors is presented in Fig. 3; as well, the shift in the corresponding Cartan tensors may be visualized by means of the Frobenius norm difference.

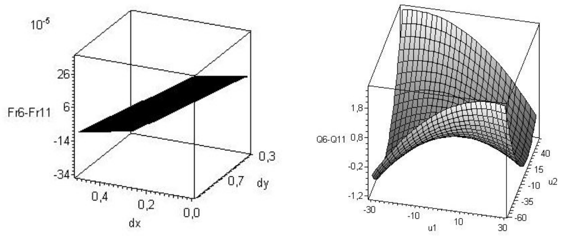

Fig. 2.: Plot of the differences between the Randers type norms and the quadratic forms for the flagpole (0.1,1).

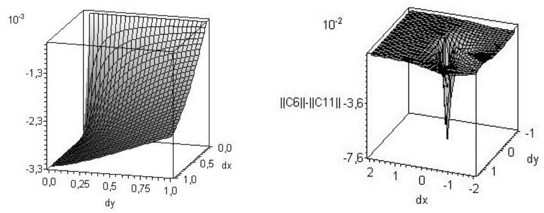

Fig. 3.: Plot of the differences between the norms of the metric and of the Cartan tensors.

5.2. THE EUCLIDEAN STRUCTURE

While considering the same grids as in the Randers cases, by means of Maple computation were produced the corresponding Euclidean structures,

$$F_{E_6}(\dot{x},\dot{y}) = \sqrt{c_1\dot{x}^2 + c_2\dot{x}\dot{y} + c_3\dot{y}^2}, \quad \begin{cases} c_1 = 0.9408054146234264 76 \\ c_2 = 1.1618981099466366898 \\ c_3 = 0.49606955256298342684\,; \end{cases}$$

$$F_{E_{11}}(\dot{x},\dot{y}) = \sqrt{c_1\dot{x}^2 + c_2\dot{x}\dot{y} + c_3\dot{y}^2}, \quad \begin{cases} c_1 = 0.9410833252243357681 \\ c_2 = 1.1625673640632761441 \\ c_3 = 0.49532779047950288618\,. \end{cases}$$

The differences between the fundamental functions and the quadratic forms are presented in Fig. 4.
The norms of the metric tensors differ by the constant

$$||g_{E_6}|| - ||g_{E_{11}}|| = 0.0000790171747404138\,,$$

and the Cartan tensors of both structures identically vanish.

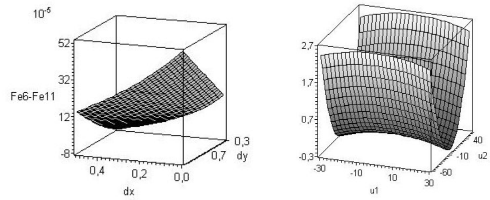

Fig. 4.: Plots of the differences between the Euclidean type norms and the quadratic forms for the flagpole $(0.1, 1)$.

5.3. THE 4-TH ROOT STRUCTURE

Similar to the previous two cases, one may consider for the two sample grids the corresponding two 4-th root structures

$$F_{Q_6}(\dot{x}, \dot{y}) = \sqrt[4]{r_6}, \qquad F_{Q_{11}}(\dot{x}, \dot{y}) = \sqrt[4]{r_{11}},$$

where

$$r_6 = a\dot{x}^4 + b\dot{x}^3\dot{y} + c\dot{x}^2\dot{y}^2 + d\dot{x}\dot{y}^3 + e\dot{y}^4, \quad \begin{cases} a = -0.320013354328217758 \\ b = 2.69642032805366582 \\ c = 2.42492765757201711 \\ d = 1.07381846633249766 \\ e = 0.254991915496320776\ , \end{cases}$$

$$r_{11} = a\dot{x}^4 + b\dot{x}^3\dot{y} + c\dot{x}^2\dot{y}^2 + d\dot{x}\dot{y}^3 + e\dot{y}^4, \quad \begin{cases} a = -0.289482051414178930 \\ b = 2.66511548305001610 \\ c = 2.43544697363887463 \\ d = 1.07031294832363754 \\ e = 0.254462441585350418\ . \end{cases}$$

The differences between the fundamental functions and between the quadratic forms for the flag $(0.1, 1)$ can be seen in Fig. 5.

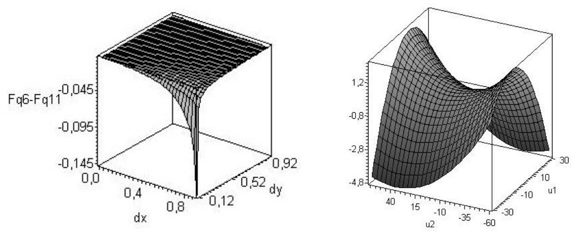

Fig. 5.: Plot of the differences between the 4−th root type norms and the quadratic forms for the flagpole $(0.1, 1)$.

The Frobenius norms of the two Cartan tensors related to the two 4-th root structures significantly differ, but have the same form (Fig. 6). All the three statistically

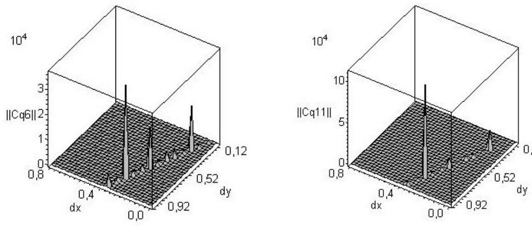

Fig. 6.: Plot of the differences between the norms of Cartan tensors

built Finslerian structures were constructed on the tangent bundle of the configuration space of the Garner dynamical system. Among them, the Randers structure explains the anisotropy of the changes of the disease progress. The Euclidean structure emphasizes the difference of the type of changes of proliferating vs. quiescent cells. The 4-th root norm $F_Q(y) = \sqrt[4]{P_4(y)}$ has its $(0,4)$ tensor induced by halving the 4-homogeneous quadratic polynomial $P_4(y)$, important for *PCA* spectral data. The norms of the related Cartan tensors give information on the degree of anisotropic character of the geometric structures. As well, the comparison of the three pairs of the same type structures (provided by grid density - variation) shows that the density increase has a significant impact especially in the case of 4-type structure, while for Euclidean type structures, the difference is very slight.

We finally note that the comparison of the rough vs. refined Finsler structures constructed for the Garner model was enabled by the standard Hilbert structure on the space of (0,2) and (0,3) Finsler-type tensors, which respectively contain the metric tensor fields (Randers, Euclidean and m-th root) and the Cartan tensor fields. The Hilbert structure allows, as well, to determine and investigate the relevance of the norms, the conformal projective factor to the standard Euclidean structure, and the deviation angle from the projection.

References

[1] P. L. Antonelli, I. Bucătaru, *New results about the geometric invariants in KCC-theory*, An.St. Univ. "Al.I.Cuza" Iasi. Mat. N.S., **47**(2001), 405–420.

[2] L. Astola, L. Florack, *Finsler Geometry on higher order tensor fields and applications to high angular resolution diffusion imaging*, Int. J. Comput. Vis., **92**(2011), 325–336. DOI 10.1007/s11263-010-0377-z

[3] V. Balan, I. R. Nicola, *Static bifurcation diagrams and the universal unfolding for cancer cell population model*, Proc. of The 9-th WSEAS International Conference on Mathematics and Computers in Biology and Chemistry (MCBC′08), Bucharest, Romania, June 24-26, 2008.

[4] V. Balan, I. R. Nicola, *Versal deformation and static bifurcation diagrams for the cancer cell population model*, Q. Appl. Math., **67**, 4(2009), 755-770.

[5] V. Balan, I. R. Nicola, *Berwald-Moor metrics and structural stability of conformally-deformed geodesic SODE*, Appl. Sci., **11**(2009), 19–34.

[6] V.Balan, J. Stojanov, *Finsler-type estimators for the cancer cell population dynamics*, to appear in Publications de l'institut Mathématique, Belgrade, 2014.

[7] V.Balan, J. Stojanov, *Statistical Finsler-Randers structures for the Garner cancer cell model*, Proceedings of RIGA 2014 (Riemannian Geometry and Applications to Engineering and Economics), May 19-21, 2014, Bucharest, Romania, Publishing House of the University of Bucharest 2015, 11-20.

[8] D. Bao, S.-S. Chern, Z. Shen, *An Introduction to Riemann-Finsler Geometry*, Graduate Texts in Mathematics 200, Springer-Verlag, 2000.

[9] I. Bucataru, R. Miron, *Finsler-Lagrange geometry. Applications to dynamical systems*, Editura Academiei Romane, Bucuresti, 2007.

[10] S.-S. Chern, Z. Shen, *Riemann-Finsler Geometry*, World Scientific, 2005.

[11] J. P. Freyer, R. M. Sutherland, *Regulation of growth saturation and development of necrosis in EMT6/R0 multicellular spheroids by the glucose and oxygen supply*, Cancer Res., **46**(1986), 3504–3512.

[12] A. L. Garner, Y. Y. Lau, D. W. Jordan, M. D. Uhler, R. M. Gilgenbach, *Implication of a simple mathematical model to cancer cell population dynamics*, Cell Prolif., **39**(2006), 15–28.

[13] A.M. Luciani, A. Rosi, P. Matarrese, G. Arancia, L. Guidoni, V. Viti, *Changes in cell volume and internal sodium concentration in HrLa cells during exponential growth and following Ionidamine treatment*, Eur. J. Cell Biol., **80**(2001), 187–195.

[14] R. Miron, M. Anastasiei, *Vector Bundles and Lagrange Spaces with Applications to Relativity*, Geometry Balkan Press, Romania, 1997.

[15] T. Reya, S. J. Morrison, M. F. Clarke, I. L. Weissman, *Stem cells, cancer, and cancer stem cells*, Nature, **414**(2001), 105–111.

[16] G.I. Solyanik, N. M. Berezetskaya, R. I. Bulkiewicz, G. I. Kulik, *Different growth patterns of a cancer cell population as a function of its starting growth characteristics: Analysis by mathematical modelling*, Cell Prolif. **28**, 5(1995), 263–278.